Twin-Timescale Beamforming for IRS-Assisted Millimeter Wave Massive MIMO-OFDM Systems

Peilan Wang¹, Zhuoran Wu¹, Jun Fang¹, and Hongbin Li²

¹ University of Electronic Science and Technology of China

² Stevens Institute of Technology

Email: peilan_wangle@gmail.com, junfang@uestc.edu.cn, Hongbin.Li@stevens.edu

Abstract—We investigate a twin-timescale joint beamforming problem for multiple intelligent reflecting surfaces (IRSs)-assisted multi-user mmWave orthogonal frequency division multiplexing (OFDM) systems, where the base station (BS) employs a hybrid analog and digital precoder. To alleviate the burden of frequent channel state information (CSI) acquisition and reduce design complexity, we devise the passive beamforming vector and the analog precoder based on statistical CSI, while the digital precoder is designed based on low-dimensional instantaneous CSI. Specifically, the former long-term optimization can be formulated as a stochastic optimization problem. To address this problem, we propose two different solutions. The first method devises the passive beamforming vector and the analog precoder by maximizing the ergodic channel gain. We also propose a deep unrolling-based method to provide a unified framework for the stochastic optimization problem. Our simulation results demonstrate the effectiveness and computational efficiency of the proposed methods.

Index Terms—Intelligent reflecting surfaces, millimeter wave communications, twin-timescale beamforming

I. INTRODUCTION

Intelligent reflecting surfaces (IRSs) have emerged as a competitive candidate for future 6G communications, owing to their ability to smartly reconfigure the wireless signal propagation environment [1]. In particular, IRSs have shown great potential in addressing the blockage issue in mmWave/THz communications through joint active and passive beamforming. However, joint beamforming design requires instantaneous channel state information (CSI), which necessitates abundant training overhead. In contrast, statistical CSI remains invariant over a long time duration and can be obtained with much lower training overhead [2]. Recent works have struck an elegant tradeoff between system performance and training overhead by leveraging two-timescale beamforming, where passive beamforming at the IRS is designed based on longterm statistical CSI, and digital precoding at the base station (BS) is optimized based on short-term instantaneous CSI of the effective BS-user channel [3], [4]. However, BS typically adopts a large-scale antenna array to combat severe path loss in mmWave/THz communications, thereby making the digital precoder design in [3], [4] computationally intensive and energy-inefficient. To address these issues, [5] considered

This work is supported in part by the National Science Foundation under Grant ECCS-1923739, ECCS-2212940, and CCF-2316865.

978-1-6654-3540-6/22 © 2023 IEEE

a *twin-timescale* beamforming approach for downlink singleuser (SU) MIMO systems with a hybrid structure. Specifically, the passive beamforming at the IRS and analog precoding at the BS are designed to maximize the upper bound of the ergodic rate, which is calculated based on statistical CSI. On the other hand, digital precoding is devised based on the instantaneous CSI of the low-dimensional equivalent channel. Despite its low complexity, the upper bound in [5] in SU-MIMO systems may result in a large condition number which is unfavorable for increasing the ergodic rate. Furthermore, the upper bound can not be readily extended to multi-user scenarios due to mutual user interference, thereby rendering long-term optimization almost intractable in such cases.

In this paper, we investigate the twin-timescale beamforming problem for multi-IRS-assisted multi-user mmWave OFDM downlink systems. We formulate the twin-timescale problem as a non-convex stochastic optimization problem and then decouple it into long-term and short-term optimization problems. By exploiting the shared statistical CSI among different subcarriers, we propose to maximize the ergodic channel gain for long-term optimization and employ a multi-ratio fractional programming (FP) algorithm for short-term optimization. Furthermore, we propose a deep unrolling-based method to provide a unified framework to address the stochastic optimization problem. Specifically, we use a deep unrolling neural network to learn the input-output relationship of the short-term optimization problem, based on which the long-term optimization variable can be trained using backpropagation techniques.

II. SYSTEM MODEL AND PROBLEM FORMULATION

A. System Model

In this paper, we consider a wideband mmWave OFDM system, where N IRSs are deployed to assist the downlink transmission from the BS with N_t antennas to K single-antenna users. To reduce the hardware cost, the BS adopts a hybrid structure with $N_{\rm RF} \ll N_t$ radio frequency (RF) chains. Let $s_{k,p}$ be the data symbol for user k, the transmitter first precodes $s_{k,p}$ at each subcarrier $p=1,\ldots,P$, using a low dimensional digital precoding vector $\boldsymbol{w}_{k,p} \in \mathbb{C}^{N_{\rm RF}\times 1}$, then transform the signal into time domain with P-point inverse discrete Fourier transforms (IDFT) followed by cyclic prefix (CP) addition at each RF chain. Subsequently, the analog precoding matrix $\boldsymbol{F}_{\rm RF} \in \mathbb{C}^{N_t \times N_{\rm RF}}$ is applied to generate the final transmitted signal. For simplicity, define $\boldsymbol{f}_{k,p} \triangleq \boldsymbol{F}_{\rm RF} \boldsymbol{w}_{k,p}$

as the effective precoding vector for user k at subcarrier p. Then, the transmitted signal at the pth subcarrier is given by $\boldsymbol{x}_p = \sum_{k=1}^K \boldsymbol{f}_{k,p} s_{k,p}$ satisfying $\|\boldsymbol{x}_p\|_2^2 \leq P_t$, where P_t is the total transmit power. Moreover, the nth IRS is a uniform planar array (UPA) with $M_n = M_{n,y} \times M_{n,z}$ passive reflecting elements. Let $\boldsymbol{\Phi}_n \triangleq \operatorname{diag}(\boldsymbol{v}_n^H)$ be the reflection phase shift matrix of the nth IRS with $\boldsymbol{v}_n \triangleq [e^{j\phi_{n,1}} \dots e^{j\phi_{n,M_n}}]^H \in \mathbb{C}^{M_n \times 1}$ denoting its passive beamforming vector and $\phi_{n,m} \in [0,2\pi)$ denoting its phase shift of the mth passive reflecting element. It should be noted that the reflection phase shift matrix is frequency flat over different subcarriers. Let $\boldsymbol{G}_n[p] \in \mathbb{C}^{M_n \times N_t}$, $\boldsymbol{r}_{n,k}[p] \in \mathbb{C}^{M_n \times 1}$, and $\boldsymbol{d}_k[p] \in \mathbb{C}^{N_t \times 1}$ denote the BS - nth IRS, nth IRS - kth user, and BS - kth user channels at subcarrier k0 in the frequency domain, respectively. Then, the effective channel between the BS and the kth user at subcarrier k1 can be characterized as

$$\boldsymbol{h}_{\text{eff},k}^{H}[p] \triangleq \sum_{n=1}^{N} \boldsymbol{r}_{n,k}^{H}[p] \boldsymbol{\Phi}_{n} \boldsymbol{G}_{n}[p] + \boldsymbol{d}_{k}^{H}[p]$$
$$= \sum_{n=1}^{N} \boldsymbol{v}_{n}^{H} \boldsymbol{H}_{n,k}[p] + \boldsymbol{d}_{k}^{H}[p], \in \mathbb{C}^{1 \times N_{t}} \qquad (1)$$

where $H_{n,k}[p] \triangleq \operatorname{diag}(r_{n,k}^H[p])G_n[p]$ represents the cascaded BS- nth IRS - kth user channel. As a result, the received signal of the kth user at subcarrier p is given by

$$y_{k,p} = \boldsymbol{h}_{\text{eff},k}^{H}[p]\boldsymbol{f}_{k,p}s_{k,p} + \boldsymbol{h}_{\text{eff},k}^{H}[p]\sum_{j\neq k}^{K} \boldsymbol{f}_{j,p}s_{j,p} + n_{k,p},$$
 (2)

where $n_{k,p} \sim \mathcal{CN}(0, \sigma_{k,p}^2)$ denotes i.i.d. complex additive white Gaussian noise. The received signal-to-interference-noise ratio (SINR) of the kth user at subcarrier p can be calculated as

$$\gamma_{k,p} = \frac{|\boldsymbol{h}_{\text{eff},k}^{H}[p]\boldsymbol{F}_{\text{RF}}\boldsymbol{w}_{k,p}|^{2}}{\sum_{j\neq k}^{K}|\boldsymbol{h}_{\text{eff},k}^{H}[p]\boldsymbol{F}_{\text{RF}}\boldsymbol{w}_{j,p}|^{2} + \sigma_{k,p}^{2}}.$$
 (3)

B. Channel Model

We adopt a geometric wideband mmWave model [6] to characterize the related channels. Specifically, the BS-nth IRS channel $G_n[p]$, the BS-kth user channel $d_k[p]$, and the nth IRS-kth user channel $r_{n,k}[p]$ in the frequency domain can be respectively characterized as

$$\boldsymbol{G}_{n}[p] = \sum_{l=1}^{L_{n}} \varrho_{n,l}^{G} \boldsymbol{a}_{r} \left(\vartheta_{n,l}^{r}, \gamma_{n,l}^{r} \right) \boldsymbol{a}_{t}^{H} \left(\phi_{n,l}^{t} \right) e^{-j2\pi f_{s} \tau_{l}^{n} \frac{p}{P}}, \quad (4)$$

$$\boldsymbol{d}_{k}\left[p\right] = \sum_{l=1}^{I_{k}} \varrho_{k,l}^{d} \boldsymbol{a}_{t}\left(\zeta_{k,l}^{t}\right) e^{-j2\pi f_{s} \iota_{l}^{k} \frac{p}{P}},\tag{5}$$

$$\boldsymbol{r}_{n,k}[p] = \sum_{l=1}^{J_{n,k}} \varrho_{n,k,l}^r \boldsymbol{a}_r \left(\vartheta_{n,k,l}^t, \gamma_{n,k,l}^t \right) e^{-j2\pi f_s \kappa_l^{n,k} \frac{p}{P}}, \tag{6}$$

where $f_s=1/T_s$ is the sampling frequency, L_n , I_k , and $J_{n,k}$ denote the number of paths of the corresponding channels, $\varrho_{i,l}^c \sim \mathcal{CN}(0,\sigma_{c,i,l}^2), c \in \{G,r,d\}, i \in \{n,k,\{n,k\}\}$ represents the associated complex path gain, a_r (a_t) denotes the normalized array response vector at the IRS (BS); $\{\tau_l^n, \iota_l^k, \kappa_l^{n,k}\}$ denotes the corresponding time delay, $\vartheta_{n,l}^r$ ($\gamma_{n,l}^r$) denotes the

azimuth (elevation) angle of arrival (AoA) of the BS-nth IRS link, $\phi_{n,l}^t$ is the associated angle of departure (AoD), $\zeta_{k,l}^t$ denotes the AoD of the BS-kth user link, and $\vartheta_{n,k,l}^t$ ($\gamma_{n,k,l}^t$) denotes the azimuth (elevation) AoD of the nth IRS-kth user link, respectively.

Based on (4)-(6), the cascaded BS-nth IRS-kth user channel $\boldsymbol{H}_{n,k}[p]$ can be further expressed as

$$\boldsymbol{H}_{n,k}[p] = \sum_{i=1}^{L_n} \sum_{j=1}^{J_{n,k}} \varrho_i^G(\varrho_j^r)^* e^{-j2\pi f_s \frac{p}{P}(\tau_i - \kappa_j)} \times \boldsymbol{a}_r \left(\vartheta_i^r - \vartheta_j^t, \gamma_i^r - \gamma_j^t\right) \boldsymbol{a}_t^H \left(\varphi_i^t\right)$$

$$\stackrel{(a)}{=} \sum_{u=1}^{U_{n,k}} \varrho_u^C e^{-j2\pi f_s \frac{p}{P}\chi_u} \boldsymbol{a}_r \left(\vartheta_u, \gamma_u\right) \boldsymbol{a}_t^H \left(\varphi_u^t\right)$$

$$\stackrel{(b)}{=} \boldsymbol{D}_{R,n,k} \boldsymbol{S}_{n,k}[p] \boldsymbol{D}_{B,n,k}^H, \tag{7}$$

where $U_{n,k} = L_n \times J_{n,k}$ and the mapping in (a) is given by [7]

$$(i-1)J_{n,k} + j \mapsto u, \ \varrho_i^G(\varrho_j^r)^* \mapsto \varrho_u^C, \ \tau_i - \kappa_j \mapsto \chi_u,$$

$$(8)$$

$$\boldsymbol{a}_{r}\left(\vartheta_{i}^{r}-\vartheta_{j}^{t},\gamma_{i}^{r}-\gamma_{j}^{t}\right)\mapsto\boldsymbol{a}_{r}\left(\vartheta_{u},\gamma_{u}\right),\ a_{t}\left(\phi_{i}^{t}\right)\mapsto a_{t}\left(\phi_{u}^{t}\right),\tag{9}$$

with $i \in \{1,2,\ldots L_n\}, \ j \in \{1,2,\ldots,J_{n,k}\};$ in (b) we define $\mathbf{D}_{\mathrm{R},n,k} \triangleq [\mathbf{a}_r(\vartheta_1,\gamma_1^r) \ \ldots \ \mathbf{a}_r(\vartheta_{U_{n,k}}^r,\gamma_{U_{n,k}}^r)] \in \mathbb{C}^{M_n \times U_{n,k}},$ $\mathbf{S}_{n,k} \triangleq \mathrm{diag}(\varrho_1^C e^{-j2\pi f_s \frac{p}{P} \chi_u},\ldots,\varrho_{U_{n,k}}^C e^{-j2\pi f_s \frac{p}{P} \chi_{U_{n,k}}}) \in \mathbb{C}^{U_{n,k} \times U_{n,k}},$ and $\mathbf{D}_{\mathrm{B},n,k} \triangleq [\mathbf{a}_t(\phi_1^t) \ \ldots \ \mathbf{a}_t(\phi_{U_{n,k}}^t)] \in \mathbb{C}^{N_t \times U_{n,k}}; \ \varrho_u^C \ \text{is the } u\text{th cascaded path gain with zero mean and variance given by } \sigma_{C,u}^2 \triangleq \mathbb{E}[|\varrho_u^C|^2] = \sigma_{G,i}^2 \sigma_{r,j}^2.$

Similarly, the BS-kth user channel $d_k[p]$ can be recast as

$$\boldsymbol{d}_{k}[p] = \boldsymbol{D}_{\mathrm{B} d_{k}} \, \boldsymbol{\beta}_{k}[p], \tag{10}$$

where $m{D}_{\mathrm{B},d_k} \triangleq [m{a}_t(\zeta_{k,1}^t) \ \dots \ m{a}_t(\zeta_{k,J_k}^t)] \in \mathbb{C}^{N_t imes I_k}$ and $m{\beta}_k \triangleq [m{\varrho}_{k,1}^d e^{-j2\pi f_s \iota_{k}^k \frac{p}{P}}]^T \in \mathbb{C}^{I_k imes 1}$.

C. Problem Formulation

As revealed by real-world mmWave channel measurements [8], the statistical channel information, including the fading channel statistics $\sigma_{c,i,l}^2$ and angle parameters such as AoA and AoD, which depend on the relative positions of the transceivers and scatters, remains invariant within tens to even hundreds of coherence blocks. Therefore, it is natural to devise the passive beamforming vector and the analog precoder based on statistical CSI in order to avoid frequent instantaneous CSI acquisition.

To strike a good balance between the training/computation resources and system performance, the analog precoder $F_{\rm RF}$ and the passive beamforming vectors $\{v_n\}$ are designed based on long-term channel statistics, which is termed *long-term* optimization. By contrast, *short-term* optimization aims to optimize the digital precoder based on the instantaneous CSI

of the reduced equivalent channel $h_{eq,k}[p]$, i.e.,

$$\tilde{\boldsymbol{h}}_{\mathrm{eq},k}^{H}[p] \triangleq (\sum_{n=1}^{N} \boldsymbol{G}_{n}^{H}[p] \mathrm{diag}(\boldsymbol{v}_{n}) \boldsymbol{r}_{n,k}[p] + \boldsymbol{d}_{k}^{H}[p]) \boldsymbol{F}_{\mathrm{RF}}. \quad (11)$$

We aim to maximize the ergodic sum rate of all subcarriers based on the twin-timescale CSI. Such a problem is formulated

$$\max_{\{\boldsymbol{v}_{n}\},\boldsymbol{F}_{\mathrm{RF}}} \quad \frac{1}{P} \mathbb{E} \left\{ \max_{\{\boldsymbol{w}_{k,p}\}} \sum_{p=1}^{P} \sum_{k=1}^{K} \log_{2} \left(1 + \gamma_{k,p} \right) \right\},$$
s.t.
$$\operatorname{Tr}(\boldsymbol{F}_{\mathrm{RF}} \boldsymbol{W}_{p} \boldsymbol{W}_{p}^{H} \boldsymbol{F}_{\mathrm{RF}}) \leq P_{t},$$

$$|\boldsymbol{F}_{\mathrm{RF}}(i,j)| = 1,$$

$$|\boldsymbol{v}_{n}(m)| = 1,$$
(12)

where $\boldsymbol{W}_{p} \triangleq [\boldsymbol{w}_{1,p},\ldots,\boldsymbol{w}_{K,p}] \in \mathbb{C}^{N_{\mathrm{RF}} \times K}, \; \boldsymbol{F}_{\mathrm{RF}}(i,j)$ is the (i,j)th element of $\boldsymbol{F}_{\mathrm{RF}},\; \boldsymbol{v}_{n}(m)$ is the mth entry of \boldsymbol{v}_{n} , the expectation is computed over the distribution of wideband mmWave channels $\{\boldsymbol{H}_{n,k}[p]\}$ and $\{\boldsymbol{d}_k[p]\}$, and $\gamma_{k,p}$ is defined in (3). The problem (12) is highly non-convex due to the coupling of optimization variables and non-convex unit modulus constraints. The long-term stochastic optimization is even more challenging because the objective function in (12) hardly admits an analytical expression. To address this issue, we propose two efficient methods based on the ergodic-channelgain-maximization (ECGM) criterion and a deep unrolling framework, respectively.

III. SHORT-TERM OPTIMIZATION

To deal with (12), suppose the analog precoder $F_{\rm RF}$ and passive beamforming vectors v_n are pre-optimized. Then, the BS can estimate the equivalent channel $h_{eq,k}[p]$ in (11) with a much lower training overhead, based on which the digital precoding vector $\boldsymbol{w}_{k,p}$ can be devised to maximize the sum rate. In particular, the short-term optimization problem can be characterized as

$$\max_{\{\boldsymbol{w}_{k,p}\}} \quad \frac{1}{P} \sum_{k=1}^{K} \log_{2} \left(1 + \frac{|\tilde{\boldsymbol{h}}_{\text{eq},k}^{H}[p] \ \boldsymbol{w}_{k,p}|^{2}}{\sum_{j \neq k}^{K} |\tilde{\boldsymbol{h}}_{\text{eq},k}^{H}[p] \ \boldsymbol{w}_{j,p}|^{2} + \sigma_{k,p}^{2}} \right),$$
s.t.
$$\sum_{k=1}^{K} \|\boldsymbol{F}_{\text{RF}} \boldsymbol{w}_{k,p}\|_{2}^{2} \leq P_{t}.$$
 (13)

It can be seen that the problem (13) is a conventional MIMO digital precoding problem that has been extensively explored in the literature. In this paper, we adopt the multi-ratio fractional programming (FP) method in [9] to obtain a suboptimal solution, in which the iteration process can be performed as

$$\alpha_{k,p} = 1 + \frac{|\tilde{\boldsymbol{h}}_{\text{eq,k}}^{H}[p] \ \boldsymbol{w}_{k,p}|^{2}}{\sum_{j\neq k}^{K} |\tilde{\boldsymbol{h}}_{\text{eq,k}}^{H}[p] \ \boldsymbol{w}_{j,p}|^{2} + \sigma_{k,p}^{2}},$$
(14)
$$\beta_{k,p} = \frac{\sqrt{1 + \alpha_{k,p}} \tilde{\boldsymbol{h}}_{\text{eq,k}}^{H}[p] \ \boldsymbol{w}_{k,p}}{\sum_{j=1}^{K} |\tilde{\boldsymbol{h}}_{\text{eq,k}}^{H}[p] \ \boldsymbol{f}_{k,p}|^{2} + \sigma_{k,p}^{2}},$$
(15)

$$\beta_{k,p} = \frac{\sqrt{1 + \alpha_{k,p}} \tilde{\boldsymbol{h}}_{\text{eq,k}}^{H}[p] \boldsymbol{w}_{k,p}}{\sum_{i=1}^{K} \left| \tilde{\boldsymbol{h}}_{\text{eq,k}}^{H}[p] \boldsymbol{f}_{k,p} \right|^{2} + \sigma_{k,p}^{2}},$$
(15)

$$\boldsymbol{w}_{k,p} = \sqrt{1 + \alpha_{k,p}} \beta_{k,p} \boldsymbol{A}^{-1} \tilde{\boldsymbol{h}}_{eq,k} [p] , \qquad (16)$$

where $\alpha_{k,p}$ and $\beta_{k,p}$ are auxiliary variables, $\boldsymbol{A} \triangleq \sum_{k=1}^{K} |\beta_{k,p}|^2 \tilde{\boldsymbol{h}}_{\mathrm{eq,k}} \left[p\right] \tilde{\boldsymbol{h}}_{\mathrm{eq,k}}^H \left[p\right] + \lambda_p \boldsymbol{F}_{\mathrm{RF}}^H \boldsymbol{F}_{\mathrm{RF}}$, and λ_p is decided by the KKT condition. The FP algorithm is guaranteed to converge to KKT point [10].

IV. LONG-TERM OPTIMIZATION: A ECG MAXIMIZATION **APPROACH**

To tackle the stochastic long-term optimization problem, we first rewrite the optimized digital precoders obtained via (13) as a function of the phase shift vectors $\{v_n\}$ and analog precoder $m{F}_{\mathrm{RF}}$, i.e., $m{w}_{k,p}^{\star} = m{g}_k(\{m{v}_n\}, m{F}_{\mathrm{RF}})$. Then, the longterm optimization problem in terms of $\{\{m{v}_n\}, m{F}_{
m RF}\}$ can be recast as

$$\max_{\{\boldsymbol{v}_n\}, \boldsymbol{F}_{\mathrm{RF}}} \frac{1}{P} \mathbb{E} \left[\sum_{p=1}^{P} \sum_{k=1}^{K} \log_2(1 + \gamma_{k,p}^{\star}) \right],$$
s.t.
$$\sum_{k=1}^{K} \|\boldsymbol{F}_{\mathrm{RF}} \boldsymbol{w}_{k,p}\|_2^2 \leq P_t$$

$$|\boldsymbol{F}_{\mathrm{RF}}(i,j)| = 1,$$

$$|\boldsymbol{v}_n(m)| = 1,$$
(17)

where

$$\gamma_{k,p}^{\star}(\{\boldsymbol{v}_n\}, \boldsymbol{F}_{\mathrm{RF}}) \triangleq \frac{|\tilde{\boldsymbol{h}}_{\mathrm{eq},k}^{H}[p] \ \boldsymbol{w}_{k,p}^{\star}|^{2}}{\sum_{j\neq k}^{K} |\tilde{\boldsymbol{h}}_{\mathrm{eq},k}^{H}[p] \ \boldsymbol{w}_{j,p}^{\star}|^{2} + \sigma_{k,p}^{2}}.$$
 (18)

Unfortunately, $\boldsymbol{w}_{k,p}^{\star}$ does not have an analytical expression in terms of $\{\boldsymbol{v}_n\}$ and $\boldsymbol{F}_{\mathrm{RF}}$. Consequently, the ergodic sum rate does not have an explicit expression of $\{v_n\}$ and $F_{\rm RF}$. To address this difficulty, we propose an effective criterion termed ergodic-channel-gain-maximization (ECGM). In particular, we optimize the long-term variables to maximize the ergodic channel gain of all users and leave the task of multi-user interference cancellation to the digital precoder. The ECGM criterion yields the following problem¹

$$\max_{\{\boldsymbol{v}_n\}, \boldsymbol{F}_{\mathrm{RF}}} \frac{1}{P} \sum_{p=1}^{P} \mathbb{E} \left[\operatorname{Tr} \left(\tilde{\boldsymbol{H}}_{\mathrm{eq}}^{H}[p] \, \tilde{\boldsymbol{H}}_{\mathrm{eq}}[p] \right) \right],$$
s.t.
$$|\boldsymbol{F}_{\mathrm{RF}}(i,j)| = 1,$$

$$|\boldsymbol{v}_n(m)| = 1,$$
(19)

where $\tilde{\boldsymbol{H}}_{\mathrm{eq}}[p] \triangleq \left[\tilde{\boldsymbol{h}}_{\mathrm{eq},1}[p] \ \dots \ \tilde{\boldsymbol{h}}_{\mathrm{eq},K}[p] \right] \in \mathbb{C}^{N_{\mathrm{RF}} \times K}$ and $h_{\text{eq},k}[p]$ is defined in (11).

So far, we have succeeded in decoupling long-term and shortterm variables. However, the analog precoder $F_{\rm RF}$ and passive beamforming vectors $\{v_n\}$ are still coupled in the objective function in (19). To solve (19), we develop an alternating optimization algorithm to alternately optimize $F_{\rm RF}$ and $\{v_n\}$.

A. Design of passive beamforming vectors $\{v_n\}$

In this subsection, we optimize the passive beamforming vector v_n while keeping the other variables fixed. The objective

¹The transmit power constraint can be satisfied by optimizing the digital precoder and is thus omitted.

function in (19) can be recast as

$$\frac{1}{P} \sum_{p=1}^{P} \mathbb{E} \left[\text{Tr} \left(\tilde{\boldsymbol{H}}_{eq}^{H}[p] \tilde{\boldsymbol{H}}_{eq}[p] \right) \right] = \boldsymbol{v}_{n}^{H} \boldsymbol{R}_{n} \boldsymbol{v}_{n} + C_{1}, \quad (20)$$

where

$$R_{n} \triangleq \frac{1}{P} \sum_{p=1}^{P} \sum_{k=1}^{K} \mathbb{E} \left[\boldsymbol{H}_{n,k}[p] \boldsymbol{F}_{RF} \boldsymbol{F}_{RF}^{H} \boldsymbol{H}_{n,k}^{H}[p] \right]$$

$$\stackrel{(a)}{=} \frac{1}{P} \sum_{p=1}^{P} \sum_{k=1}^{K} \mathbb{E} \left[\boldsymbol{D}_{R,n,k} \boldsymbol{S}_{n,k}[p] \boldsymbol{Q}_{n,k} \boldsymbol{S}_{n,k}^{H}[p] \boldsymbol{D}_{R,n,k}^{H} \right]$$

$$\stackrel{(b)}{=} \sum_{k=1}^{K} \boldsymbol{D}_{R,n,k} \boldsymbol{\Sigma}_{n,k} \boldsymbol{D}_{R,n,k}^{H} \in \mathbb{C}^{M_{n} \times M_{n}}, \qquad (21)$$

where in (a), we define $Q_{n,k} \triangleq D_{\mathrm{B},n,k}^H F_{\mathrm{RF}} F_{\mathrm{RF}}^H D_{\mathrm{B},n,k}$; in (b) we define

$$\Sigma_{n,k} \triangleq \mathbb{E}[\boldsymbol{S}_{n,k}[p] \, \boldsymbol{Q}_{n,k} \boldsymbol{S}_{n,k}^{H}[p]]$$

$$= \operatorname{diag}(\boldsymbol{Q}_{n,k}(1,1) \sigma_{C,1}^{2} \dots \boldsymbol{Q}_{n,k}(U_{n,k}, U_{n,k}) \sigma_{C,U_{n,k}}^{2}) \quad (22)$$

where $Q_{n,k}(i,j)$ is the (i,j)th entry of $Q_{n,k}$ and $\Sigma_{n,k}$ is flat to all subcarriers; C_1 is a constant irrespective of v_n . Then, the optimization problem of v_n can be expressed as

$$\max_{\boldsymbol{v}_n} \quad \boldsymbol{v}_n^H \boldsymbol{R}_n \boldsymbol{v}_n, \quad \text{s.t.} \quad |\boldsymbol{v}_n(m)| = 1,$$
 (23)

In spite of the non-convex unit modulus constraints, the problem (23) can be efficiently solved via manifold optimizationbased algorithms [4], where the detailed procedures are omitted for brevity.

B. Design of analog precoder F_{RF}

In this subsection, we optimize the analog precoder F_{RF} by fixing the passive beamforming vectors $\{v_n\}$. The objective function in (19) can be recast as

$$\frac{1}{P} \sum_{p=1}^{P} \mathbb{E} \left[\operatorname{Tr} \left(\tilde{\boldsymbol{H}}_{eq}^{H}[p] \, \tilde{\boldsymbol{H}}_{eq}[p] \right) \right]
= \frac{1}{P} \sum_{p=1}^{P} \mathbb{E} \left[\operatorname{Tr} \left(\boldsymbol{F}_{RF}^{H} \boldsymbol{H}_{eff}[p] \boldsymbol{H}_{eff}^{H}[p] \boldsymbol{F}_{RF} \right) \right] + C_{2}
= \operatorname{Tr} \left(\boldsymbol{F}_{RF}^{H} \overline{\boldsymbol{R}} \boldsymbol{F}_{RF} \right) + C_{2},$$
(24)

where $\overline{\boldsymbol{R}} \triangleq 1/P\sum_{p=1}^{P} \mathbb{E}\big[\boldsymbol{H}_{\mathrm{eff}}[p]\boldsymbol{H}_{\mathrm{eff}}^{H}[p]\big] \in \mathbb{C}^{N_{t}\times N_{t}}$ and $\boldsymbol{H}_{\mathrm{eff}} \triangleq [\boldsymbol{h}_{\mathrm{eff},1},\ldots,\boldsymbol{h}_{\mathrm{eff},K}] \in \mathbb{C}^{N_{t}\times K}$; C_{2} is a constant irrespective of $\boldsymbol{F}_{\mathrm{RF}}$. Moreover, the covariance matrix $\overline{\boldsymbol{R}}$ can be calculated as

$$\overline{R} = \frac{1}{P} \sum_{p=1}^{P} \mathbb{E} \left[\boldsymbol{H}_{\text{eff}}[p] \boldsymbol{H}_{\text{eff}}^{H}[p] \right]
= \sum_{k=1}^{K} \left(\boldsymbol{D}_{B,d_{k}} \overline{\boldsymbol{B}}_{k} \boldsymbol{D}_{B,d_{k}}^{H} + \sum_{n=1}^{N} \boldsymbol{D}_{B,n,k} \overline{\boldsymbol{V}}_{n,k} \boldsymbol{D}_{B,n,k}^{H} \right),$$
(25)

 $\begin{array}{lll} \text{where} & \overline{\boldsymbol{B}}_k & \triangleq & \mathbb{E}[\boldsymbol{\beta}_k[p]\boldsymbol{\beta}_k^H[p]] & = & \operatorname{diag}(\sigma_{d,k,1}^2,\ldots,\sigma_{d,k,I_k}^2), \\ \overline{\boldsymbol{V}}_{n,k} & \triangleq & \operatorname{diag}(c_1,\ldots,c_{U_{n,k}}), & c_u & \triangleq & \sigma_{C,u}^2\boldsymbol{V}_{n,k}(u,u), \text{ and } \\ \boldsymbol{V}_{n,k} & \triangleq & \boldsymbol{D}_{\mathrm{R},n,k}^H \boldsymbol{\mathbf{D}}_{\mathrm{R},n,k}. \end{array}$

Then, the optimization problem of $oldsymbol{F}_{\mathrm{RF}}$ can be characterized as

$$\max_{\boldsymbol{F}_{RF}} \operatorname{Tr}(\boldsymbol{F}_{RF}^{H} \overline{\boldsymbol{R}} \boldsymbol{F}_{RF}), \quad \text{s.t.} \quad |\boldsymbol{F}_{RF}(i,j)| = 1.$$
 (26)

Without the unit modulus constraint $|F_{\rm RF}(i,j)|=1$, the problem is a generalized eigenvalue problem, and its optimal solution can be obtained by SVD. Denote its eigenvalue decomposition as $\overline{R}=U\overline{\Sigma}U^{\rm H}$. Then, the optimal $F_{\rm RF}$ without constraint is given by $F_{\rm RF}^*=U(:,1:N_{\rm RF})T$, where $U(:,1:N_{\rm RF})$ denotes the submatrix comprising its $N_{\rm RF}$ eigenvectors associated first largest $N_{\rm RF}$ eigenvalues and $T\in\mathbb{C}^{N_{\rm RF}\times N_{\rm RF}}$ is an arbitrary non-singular matrix. Then, we obtain a near-optimal by projecting $F_{\rm RF}^*$ onto the manifold $|F_{\rm RF}(i,j)|=1$, i.e., $F_{\rm RF}^*=\exp(1j\angle U(:,1:N_{\rm RF}))$.

By alternately optimizing F_{RF} and $\{v_n\}$, the algorithm can converge to a critical point of the problem (19).

It is observed from (23) and (26) that the design of passive beamforming vectors $\{v_n\}$ and the analog precoder F_{RF} depends only on spatial correlation matrices $R_{n,k}$ and \overline{R} which vary much more slowly than instantaneous CSI. Briefly speaking, the long-term design of F_{RF} and $\{v_n\}$ aims to maximize the overall ergodic channel gain without considering multi-user interference while the short-term design of $\{w_{k,p}\}$ aims to cancel multi-user interference and maximize the sum rate.

V. LONG-TERM OPTIMIZATION: A DEEP UNROLLING-BASED APPROACH

As discussed earlier, the main obstacles to solving the long-term stochastic optimization (17) include 1) The challenge in calculating the expectation in the objective function in (17); 2) The difficulty in obtaining analytic expression of $\boldsymbol{w}_{k,p}^*$ in terms of $\{\{\boldsymbol{v}_n\}_{n=1}^N, \boldsymbol{F}_{\text{RF}}\}$. To address the first issue, we adopt the well-known sample average approximation [11] to simplify the objective function. Specifically, denote $\mathcal{H}_{\text{sam}} \triangleq \{\{\{\boldsymbol{r}_{n,k}^t[p]\}_{k=1}^K, \boldsymbol{G}_n^t[p], \{\boldsymbol{d}_k^t[p]\}_{k=1}^K\}_{p=1}^P\}_{t=1}^T$ as a set of i.i.d. wideband channel samples whose statistical characteristics are in accordance with the known statistical CSI of actual channels. Hence, the expectation in (17) can be approximated by

$$\frac{1}{P} \mathbb{E} \left[\sum_{k=1}^{K} \sum_{p=1}^{P} \log_2(1 + \gamma_{k,p}^{\star}) \right]
\approx \frac{1}{TP} \sum_{t=1}^{T} \sum_{k=1}^{K} \sum_{p=1}^{P} \log_2(1 + \gamma_{k,p,t}^{\star}),$$
(27)

where

$$\gamma_{k,p,t}^{\star}(\{\boldsymbol{v}_n\},\boldsymbol{F}_{\mathrm{RF}}) \triangleq \frac{|(\tilde{\boldsymbol{h}}_{\mathrm{eq},k}^t[p])^H (\boldsymbol{w}_{k,p}^t)^{\star}|^2}{\sum_{j\neq k}^K |(\tilde{\boldsymbol{h}}_{\mathrm{eq},k}^t[p])^H (\boldsymbol{w}_{j,p}^t)^{\star}|^2 + \sigma_{k,p}^2},$$
(28)

in which $(\tilde{\boldsymbol{h}}_{\mathrm{eq},k}^t)^H[p]$ can be obtained as (11) by adding superscript t and $(\boldsymbol{w}_{k,p}^t)^\star$ denotes the associated optimized digital precoding vector. According to the law of large numbers, the approximation error would vanish when T is sufficiently large.

On the other hand, a deep unrolling neural network (DU-NN) has proven to be highly efficient to address the latter issue [4]. Specifically, the deep unrolling neural network can unfold the traditional iterative algorithms into a layer-wise

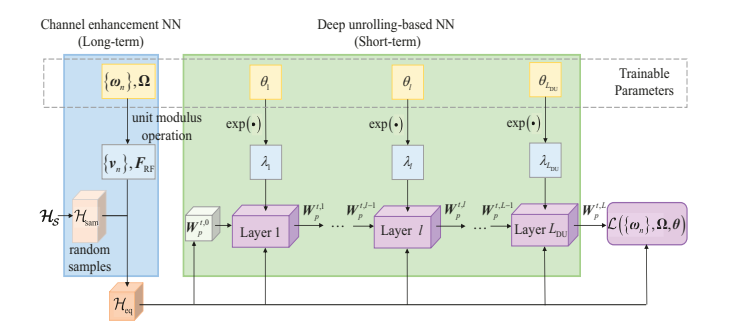


Fig. 1. The NN presentation of the proposed deep unrolling-based neural network

structure and learn the mapping between the channel sample $\tilde{\boldsymbol{H}}_{\mathrm{eq}}^t[p] \triangleq \left[\tilde{\boldsymbol{h}}_{\mathrm{eq,1}}^t[p], \ldots, \tilde{\boldsymbol{h}}_{\mathrm{eq,K}}^t[p]\right]$ and the optimal digital precoding matrix $(\boldsymbol{W}_p^t)^\star \triangleq [\boldsymbol{w}_{1,p}^\star, \ldots, \boldsymbol{w}_{K,p}^\star]$ through end-to-end training. After the mapping is learned, the relationship between $(\boldsymbol{W}_p^t)^\star$ and $\tilde{\boldsymbol{H}}_{\mathrm{eq}}^t[p]$ can be further characterized by a neural network in terms of long-term parameters $\{\{\boldsymbol{v}_n\}, \boldsymbol{F}_{\mathrm{RF}}\}$. In this case, the long-term optimization variables $\{\{\boldsymbol{v}_n\}, \boldsymbol{F}_{\mathrm{RF}}\}$ can be trained via backpropagation techniques. In the following, we elaborate on the details of the network structure.

A. Network structure

As illustrated in Fig. 1, the overall NN consists of a channel enhancement NN (CENN) that accounts for long-term optimization, a deep unrolling-based NN (DUNN) unfolding the FP algorithm for short-term optimization, and a loss function.

The CENN is responsible for generating the channel samples $\mathcal{H}_{\mathrm{sam}}$ and converting them into equivalent channel samples $\{\tilde{\boldsymbol{h}}_{\mathrm{eq},k}^t[p]\}_{k=1,p=1,t=1}^{K,P,T}$, which can be parameterized by long-term variables, i.e., $(\tilde{\boldsymbol{h}}_{\mathrm{eq},k}^t)^H[p] \triangleq (\sum_{n=1}^N (\boldsymbol{G}_n^t[p])^H \mathrm{diag}(\boldsymbol{v}_n) \boldsymbol{r}_{n,k}^t[p] + (\boldsymbol{d}_k^t)^H[p]) \boldsymbol{F}_{\mathrm{RF}}$. In order to ensure that vectors $\{\boldsymbol{v}_n\}$ and the matrix $\boldsymbol{F}_{\mathrm{RF}}$ satisfy the unit modulo constraints, we introduce corresponding auxiliary vectors $\{\boldsymbol{\omega}_n\}$ and matrix $\boldsymbol{\Omega}$ as trainable parameters. After these parameters are trained, the passive beamforming vectors $\{\boldsymbol{v}_n\}$ and $\boldsymbol{F}_{\mathrm{RF}}$ can be obtained by implementing entry-wise modulo operations, i.e., $\boldsymbol{v}_n(m) = \frac{\boldsymbol{\omega}_n(m)}{|\boldsymbol{\omega}_n(m)|}$ and $\boldsymbol{F}_{\mathrm{RF}}(i,j) = \frac{\boldsymbol{\Omega}(i,j)}{|\boldsymbol{\Omega}(i,j)|}$.

On the other hand, the main goal of the deep unrolling-based NN (DUNN) is to learn the complex dependencies between the optimal digital precoder $(\boldsymbol{W}_p^t)^\star$ and equivalent channel samples $\tilde{\boldsymbol{H}}_{eq}^t[p]$. Specifically, DUNN unfolds each iteration of the original FP algorithm, as shown in (14)-(16), into a layer in the DUNN. Each iteration depends on the Lagrangian multiplier λ_p^t which is then transferred into a series of network parameters $\{\lambda_l\}_{l=1}^L$, where L denotes the total number of layers of the DU-NN. It should be mentioned that these parameters $\{\lambda_l\}_{l=1}^L$ are flat to all channel samples and subcarriers to reduce the dimension of trainable parameters, which, even so, can achieve decent performance as will be shown in the simulation results. To assure $\lambda_l \geq 0$, we introduce auxiliary variables $\mathcal{G} \triangleq \{\theta_l\}_{l=1}^L$ as actual trainable parameters and let $\lambda_l = e^{\theta_l}$. At first, the precoding matrix $\boldsymbol{W}_p^{t,l=0}$ for

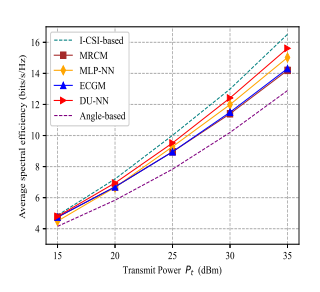
each subcarrier is initialized based on the maximum-ratio-transmission strategy. Then, the equivalent channel samples and the optimized precoding matrix $\boldsymbol{W}_p^{t,l}$ in the lth layer are fed into the l+1th layer, whose output is the optimized precoder $\boldsymbol{W}_p^{t,l+1}$. In each layer, the precoding matrix $\boldsymbol{W}_p^{t,l}$ is updated with the trainable parameters $\{\lambda_l\}_{l=1}^L$ according to (14)-(16). To satisfy the transmit power constraint and prevent gradient explosion during the training, a scaling factor is applied to the precoding matrix such that its norm square does not exceed the maximum transmit power. Through end-to-end training, the DUNN learns the trainable parameters $\{\lambda_l\}_{l=1}^L$ and finally outputs the optimal digital precoder $(\boldsymbol{W}_p^t)^\star$.

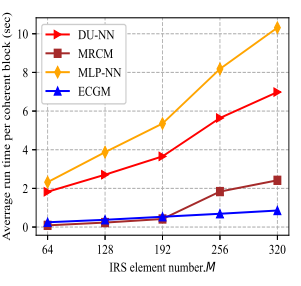
As for the loss function, we can utilize sample average approximation (27) to simplify the objective function in (17). Moreover, note that channels at different subcarriers share the same channel statistics including angle parameters and variance of path gains, we can generate a small batch size of channel samples with a limited number of subcarriers, say B < T and $P_0 < P$, to further reduce the computational complexity. In addition, the vectors $\{w_n\}$, matrix Ω , and variables G are treated as the actual trainable network parameters, i.e., $\mathcal{B} \triangleq \{\{\omega_n\}_{n=1}^N, \Omega, \mathcal{G}\}$. As a result, the loss function of the proposed DU-NN can be recast as $\tilde{\mathcal{L}}(\mathcal{B}; \mathcal{H}_{sam}) =$ $-\frac{1}{BP_0}\sum_{t=1}^{B}\sum_{k=1}^{K}\sum_{p=1}^{P_0}\log_2(1+\gamma_{k,p,t}^{\star})$, where $\gamma_{k,p,t}^{\star}$ is defined in (28). After the establishment of the network architecture, the loss function's stochastic gradient with respect to the trainable parameters ${\cal B}$ is calculated based on the chain rule during the backpropagation stage. Subsequently, the Amsgrad optimizer is utilized to update the values of the trainable parameters. In this way, the proposed DU-NN can achieve better performance than the traditional FP algorithm while inheriting the interpretability from the iteration procedure.

VI. SIMULATION RESULTS

In this section, we evaluate the performance of our proposed methods. We consider N=2 IRSs to assist the downlink transmission, which are deployed at (50, 20, 3) m and (50, -20, 3)m, respectively. The BS is located at (0,0,25) m while K=2users are randomly distributed within a circle centered at (50,0,3) m with a radius of 10 m. We assume that BS-nth IRS links and nth IRS- kth user links are LOS dominated whose Rician factors are set to 7 dB and 10 dB, respectively; by contrast, the BS-kth user links comprise only NLOS paths. The variances of complex path gain for LOS and NLOS scenarios are based on the path loss model for Urban macro (UMa) in 3GPP TR 38.901 [12]. Also, each coherence interval consists of $T_s = 40$ time slots. The noise power is set as -90 dBm. The central carrier frequency is set to 30 GHz and the sampling rate is set to $f_s = 0.08$ GHz, with time delays drawn from a uniform distribution $\mathcal{U}(0, 100)$ ns. The total number of OFDM subcarriers is set to P=32. We set L=2 and the learning rate 0.75 for fast convergence. For training efficiency, we set $P_0 = 2$ and B = 10 during the training process.

The proposed methods are termed ECGM and DU-NN, respectively. Moreover, the state-of-the-art methods [5], [10], [13] can be extended to the considered scenarios as benchmarks, i.e.,





- (a) Average sum rate versus the transmit power P_t .
- (b) Average run time versus M with $N_t = 64$.

Fig. 2. Average sum rate and average run time comparison.

- I-CSI-based: The joint optimization method based on the perfect instantaneous CSI [10].
- MRCM: The multiple-reflection coefficient matrix (MRCM) algorithm is adopted to optimize analog precoder F_{RF} based on statistical-CSI [5] while the short-term optimization is based on FP algorithm.
- MLP-NN: The "black-box" multi-layer perceptron (MLP) NN is built for short-term optimization while the longterm optimization is optimized by the proposed DU-NN.
- Angle-based: The analog precoder $F_{\rm RF}$ is designed to align the largest $N_{\rm RF}$ path in terms of the magnitude of path gains [13] while the short-term optimization is based on FP algorithm.

In Fig. 2 (a), we plot the average sum rate of respective methods as a function of the transmit power P_t , where we set $N_t=64,~N_{\rm RF}=4,~{\rm and}~M_n=16\times16=256.$ It can be observed that the proposed ECGM performs much better than the angle-based method [13] thereby demonstrating the efficacy of the criterion. Also, the performance of the proposed ECGM method nearly coincides with that of the MRCM method which also aims to maximize the ergodic equivalent channel power in essence. Moreover, it is seen that the proposed DU-NN outperforms other benchmarks based on twin-timescale CSI and the performance gap becomes more evident when the transmit power P_t increases. Additionally, the proposed DU-NN can achieve performance close to that of the I-CSI-based method with only a slight performance loss. On the other hand, long-term optimization is computationally more demanding. To further investigate the computational complexity of the algorithms, we present the average run time as a function of the number of reflecting elements M, where we fix $M_u = 16$ but increase M_z , and set $P_t = 30$ dBm. Notably, the anglebased method admits a closed-form solution and thus requires negligible time, hence, it is not depicted in the figure. Our results demonstrate that the proposed DU-NN method is more computationally efficient than the MLP-NN method, indicating the superiority of the deep unrolling technique over traditional MLP-NNs. Also, both the MRCM and the proposed ECGM method require considerably less time than other methods when $M \leq 192$. However, the MRCM method exhibits a sharp increase in computation time when $M \geq 256$, while the

proposed ECGM method remains nearly constant. One possible explanation could be that the MRCM method updates the phase shifts of each individual IRS element-by-element, which would result in a remarkable increase in time consumption when M increases. As a result, the proposed ECGM method is the most computationally efficient among the considered methods except the angle-based method.

VII. CONCLUSION

In this paper, we investigated the twin-timescale beamforming of IRSs and hybrid precoders in multi-user mmWave OFDM systems. To tackle this stochastic optimization problem, we proposed two methods: the computationally efficient ECGM method and the performance-wise superior DU-NN. Our simulation results demonstrate the competitiveness of the proposed methods in terms of spectral efficiency and computational complexity. Moreover, our proposed framework exhibits promising prospects in generalizing to more complex scenarios.

REFERENCES

- S. Zhang and R. Zhang, "Capacity characterization for intelligent reflecting surface aided MIMO communication," *IEEE J. Sel. Areas Commun.*, vol. 38, no. 8, pp. 1823–1838, Aug. 2020.
- [2] H. Wang, J. Fang, H. Duan, and H. Li, "Spatial channel covariance estimation and two-timescale beamforming for IRS-assisted millimeter wave systems," *IEEE Trans. Wireless Commun., Early Access*, 2023.
- [3] M.-M. Zhao, Q. Wu, M.-J. Zhao, and R. Zhang, "Intelligent reflecting surface enhanced wireless networks: Two-timescale beamforming optimization," *IEEE Trans. Wireless Commun.*, vol. 20, no. 1, pp. 2–17, Jan. 2021.
- [4] P. Wang, J. Fang, Z. Wu, and H. Li, "Two-timescale beamforming for IRS-assisted millimeter wave systems: A deep unrolling-based stochastic optimization approach," in *Proc. IEEE Sensor Array Multichannel Signal Process. Workshop (SAM)*, Trondheim, Norway, 2022, pp. 191–195.
- [5] F. Yang, J.-B. Wang, H. Zhang, M. Lin, and J. Cheng, "Multi-IRS-Assisted mmWave MIMO Communication Using Twin-Timescale Channel State Information," *IEEE Trans. Commun.*, vol. 70, no. 9, pp. 6370–6384, 2022.
- [6] A. Alkhateeb and R. W. Heath, "Frequency selective hybrid precoding for limited feedback millimeter wave systems," *IEEE Trans. Commun.*, vol. 64, no. 5, pp. 1801–1818, 2016.
- [7] X. Zheng, P. Wang, J. Fang, and H. Li, "Compressed channel estimation for IRS-assisted millimeter wave OFDM systems: A low-rank tensor decomposition-based approach," *IEEE Wireless Commun. Lett.*, vol. 11, no. 6, pp. 1258–1262, Jun. 2022.
- [8] A. Adhikary, E. Al Safadi, M. K. Samimi, R. Wang, G. Caire, T. S. Rappaport, and A. F. Molisch, "Joint spatial division and multiplexing for mm-wave channels," *IEEE J. Sel. Areas Commun.*, vol. 32, no. 6, pp. 1239–1255, June 2014.
- [9] K. Shen and W. Yu, "Fractional programming for communication systems—part I: Power control and beamforming," *IEEE Trans. Signal Process.*, vol. 66, no. 10, pp. 2616–2630, 2018.
- [10] H. Guo, Y.-C. Liang, J. Chen, and E. G. Larsson, "Weighted sumrate maximization for reconfigurable intelligent surface aided wireless networks," *IEEE Trans. Wireless Commun.*, vol. 19, no. 5, pp. 3064– 3076, May 2020.
- [11] K. Healy and L. W. Schruben, "Retrospective simulation response optimization," in *Proc. 23rd Conf. Winter Simul.*, ser. WSC '91. USA: IEEE Computer Society, 1991, p. 901–906.
- [12] 3GPP, "Studay on channel model for frequencies from 0.5 to 100 GHz," 3rd Generation Partnership Project (3GPP), Tech. Rep. TR 38.901 V14.1.1 Release 14, Aug. 2017. [Online]. Available: http://www.3gpp.org/DynaReport/38901.html.
- [13] J. Tan, L. Dai, J. Li, and S. Jin, "Angle-based codebook for low-resolution hybrid precoding in millimeter-wave massive MIMO systems," in *Proc. IEEE/CIC Int. Conf. Commun. China (ICCC)*, 2017, pp. 1–5.